Supporting Information

Near perfect head-to-head selectivity on the supramolecular photocyclodimerisation of 2-anthracenecarboxylate with self-organised gemini surfactant bilayers

Wijak Yospanya,[ab] Masaki Nishijima,[b] Yasuyuki Araki,[b] Thierry Buffeteau,[c] Emilie Pouget,[a] Takehiko Wada *[b] and Reiko Oda *[a]

[a] *Institute of Chemistry & Biology of Membranes & Nanoobjects (UMR5248 CBMN), CNRS – Université de Bordeaux – Bordeaux INP, 2 rue Robert Escarpit, 33607 Pessac, France.*
[b] *Institute of Multidisciplinary Research for Advanced Materials, Tohoku University, 2-1-1, Katahira, Aoba-ku, Sendai 980-8577, Japan.*
[c] *Institut des Sciences Moléculaires (UMR5255 ISM), CNRS – Université de Bordeaux, 351 Cours de la Libération, 33405 Talence, France*

Contents

Materials

All the chemicals used were of reagent or higher grade and purchased from FUJIFILM Wako Pure Chemical Corporation (Osaka, Japan), Tokyo Chemical Industry Co., Ltd. (Tokyo, Japan), and Sigma-Aldrich, Inc. (St. Louis, Missouri, USA) unless stated otherwise. The MilliQ water mentioned in this document was deionised water purified by Milli-Q® Ultrapure Water System with an electrical resistance of 18.2 Ω. The details of equipment are explained in the methods section.

Methods

Synthesis of Hybrid Silica-Organic Nanoribbons

The **16-2-16** L- or D-tartrate was dissolved in water to the final concentration of 1 mM. The solution was heated to 70 °C in a water bath for 5 min, sonicated in a sonication bath for 2 min and heated again for 5 min. If the volume of solution was more than 5 mL, it was divided to 5 mL portions and placed in 15 centrifuge tubes while heating in a water bath. The solution was cooled and aged at 20 °C in a temperature-controlled chamber. Tetraethyl orthosilicate (TEOS) (5% v/v) pre-hydrolysed for 5 h in an aqueous tartaric acid solution (0.1 mM) was transferred to the **16-2-16**-tartrate-aging tube after 1 h with the same volume as aging solution. The resulting solution was mixed by gentle inversed-shaking to avoid breaking the formed organic nanoribbons. The solution was aged for 14 h on a roller mixer at 20 °C. The hybrid nanoribbon aggregates could be observed. The solution was centrifuged at 3893×g and 4 °C for 12 min, and the supernatant was disposed to remove the excess of hydrolysed TEOS and quench the silica formation. To completely remove the excess TEOS, the precipitated get was washed 4 times in the following procedure. The gel was re-dispersed in water at 4 °C 14 mL by vortexing and sonicating 1 min in ice bath, the suspension was centrifuged at 3893×g and 4 °C for 12 min, and the supernatant was disposed. After washing, the nanostructures were re-dissolved in 5 mL (or less) of water at 4 °C. The suspension was sonicated by the probe sonicator for 5 s for two times to make a homogeneous suspension. The concentration was determined by lyophilisation of 200 µL sample. The morphology was confirmed by TEM, and the organisation of **16-2-16** tartrate was observed by CD.

Titration of Hybrid Nanoribbons with 2-Anthracenecarboxylate

ACH powder was dissolved in 1 mM aqueous NaOH solution. The solution was sonicated using a probe sonicator for 5 min in an ice bath. The solution was filtered by a 0.25 µM membrane filter unit. The concentration of AC was determined by monitoring the UV-Vis absorbance at 387 nm (ε_{max} = 3500 M^{-1} cm^{-1}).

The AC stock solution prepared above was added to the hybrid nanoribbons and diluted to the desired concentration at the designated temperature. For the CD measurement, 3 mL of each sample was prepared and incubated on a roller mixer. The lowest concentration of hybrid nanoribbons was prepared at 100 µM to avoid the critical micelle concentration problems, and the samples were diluted to the desired concentration before CD measurement. All samples used for the measurements of the same series of spectra were prepared from the same stock solutions of AC and hybrid nanoribbons with a 20 min

interval, which is the time for each CD measurement, ensuring comparable incubation time for the same set of experiment.

Circular Dichroism Spectroscopy

The J-815 instrument (JASCO, Japan) used for CD spectral measurements was equipped with a single position Peltier cell holder for temperature control. The suspension sample was diluted to the designated concentration to make a minimum volume of 2 mL in 1 × 1 x 4.5 cm quartz cuvette with stirrer bar. The measurement was conducted by setting the scan speed at 100 nm/min, the bandwidth at 2.00 nm, data integration time 0.5 s, standard sensitivity, accumulation 4 times at 4 °C while stirring (unless noted). All the data discussed in this work has linear dichroism (LD) less than 0.001 and high tension (HT) less than 600 V to ensure the identity of the CD signal.

Fluorescence Spectroscopy

Fluorescence spectra were measured with a CPL-300 spectrometer (JASCO, Japan). A 2 mL sample solution was placed in a 1 × 1 x 4.5 cm quartz cuvette equipped with a stirrer bar at the bottom. The sample chamber was cooled to 4 °C, and the sample was always stirred. The excitation wavelength was set to 350 nm, the excitation and emission bandwidth were set to 10 nm, and the monitoring wavelength was scanned from 380 to 540 nm at a 100 nm/min scan speed. For accurate comparison of the fluorescence intensity, the photomultiplier HT was set to 800 V for both the AC and AC-incorporated nanoribbon samples and the single scan mode was employed. For the photoreaction kinetic study, the samples were scan repeatedly. The photomultiplier HT was set to 700 and 850 V for AC and AC in hybrid nanoribbons to give the best quality of fluorescence intensity.

Infrared and Vibrational Circular Dichroism Spectroscopy.

Infrared (IR) and vibrational circular dichroism (VCD) spectra were recorded with a ThermoNicolet Nexus 670 FTIR spectrometer equipped with a VCD optical bench.[1] In this optical bench, the light beam was focused on the sample by a BaF_2 lens (191 mm focal length), passing an optical filter (1850-800 cm^{-1}), a BaF_2 wire grid polariser (Specac), and a ZnSe photoelastic modulator (Hinds Instruments, Type II/ZS50). The light was then focused by a ZnSe lens (38.1 mm focal length) onto a 1 × 1 mm^2 HgCdTe (ThermoNicolet, MCTA* E6032) detector. IR absorption and VCD spectra were recorded at a resolution of 4 cm^{-1}, by coadding 50 scans and 24000 scans (8h acquisition time), respectively.

The samples of hybrid nanoribbons were prepared by exchanging of D- or L-tartrate with AC in different proportions in 5 mL water at 4 °C overnight. The suspensions were centrifuged at 3893×g and 4 °C for 10 min. The supernatant of each sample was removed, and the gel was washed twice with 5 mL D_2O at 4 °C. The samples were held in a demountable CaF_2 cell (Biotools) with a fixed path length of 55 μm. In order to compare the IR spectra and to ensure the consistency of the gel in the cell, the IR spectra were normalised with respect to the 2919 cm^{-1} band related to the antisymmetric (ν_aCH_2) stretching vibration of the methylene groups of **16-2-16**.

Additional IR and VCD spectral measurements were performed for L-hybrid nanoribbons and 9-anthracenecarboxylate-exchanged L-hybrid nanoribbons (1 : 1) as well as IR spectrum of sodium salt of AC. Baseline corrections of the VCD spectra were performed by subtracting the raw VCD spectra of the

D_2O solvent. The photoelastic modulator was adjusted for a maximum efficiency in the mid-IR region at 1400 cm^{-1}. Calculations were performed via the standard ThermoNicolet software, using Happ and Genzel apodisation, de-Haseth phase-correction and a zero-filling-factor of one. Calibration spectra were recorded using a birefringent plate (CdSe) and a second BaF_2 wire grid polariser, following the experimental procedure previously published.[2] IR spectra were shown with solvent absorption subtracted out.

Transmitted Electron Microscope Measurement

The TEM sample was prepared using blotting technique. The 400-mesh carbon-coated copper grids (DELTA Microscopies, France) were used. First, the carbon side of the grid was hydrophilised by UV/Ozone ProCleaner 220 for 20 - 30 min. After that, the suspension containing nanostructures 8 µL was dropped on the carbon surface. After 1 min, the excess liquid was blotted using filter paper. In the case of organic nanostructures, uranyl acetate 2 % w 8 µL was dropped and blotted after 1 min. The surface was dried at the room temperature. The TEM images were taken from Philips CM-120 20-120 kV (FEI Company, USA). The ImageJ software (NIH and University of Wisconsin) was used to edit or scale the images.

Photocyclodimerisation of 2-Anthracenecarboxylate Mediated by Hybrid Nanoribbons

The water used for AC stock preparation and dilution in photocyclodimerisation was bubbled with N_2 gas for at least 1 h. The hybrid nanoribbons were diluted and the AC stock was added to the suspension to the desired concentration and volume. If the temperature is 4 °C, all the components were cooled in ice bath or refrigerator before mixing. The suspension was incubated before irradiation at 352 nm by an 8-W F8T5BL lamp (Ushio) under the designated conditions.

After irradiation, the suspension was centrifuged at 3893×g and 4 °C for 20 min. The supernatant was removed, and the gel was washed twice with water at 4°C of the same volume as the removed supernatant. The hydrogel obtained from the last centrifugation was lyophilised to remove water completely. Methanol (4 mL) was added to the dried hybrid nanostructures. The suspension was heated at 50 °C for 10 min and sonicated for 10 min. The suspension was centrifuged at 3893×g and 25 °C for 20 min. The supernatant (3 mL) was separated, filtered and dried in the oven to obtain the powder for HPLC analysis.

The powder containing ACDs were dissolved in aqueous NaOH (10 mM). The same volume of acetonitrile was added, and the sample was filtered through a 0.45 µM pore size filter unit. Regarding the previous report, the sample was injected to the HPLC equipped with fluorescence detector (JASCO HPLC System, Column $5C_{18}$-MS-II 4.6ID × 150 mm and CHIRALCEL OJ-RH 2.1ID × 120 mm, Injection 20 µL, Solvent acetonitrile 36 % in water containing TFA 0.1 %, Flow rate 0.5 mL / min, Fluorescence excitation 254 nm and detection 420 nm) (Fig. S1).

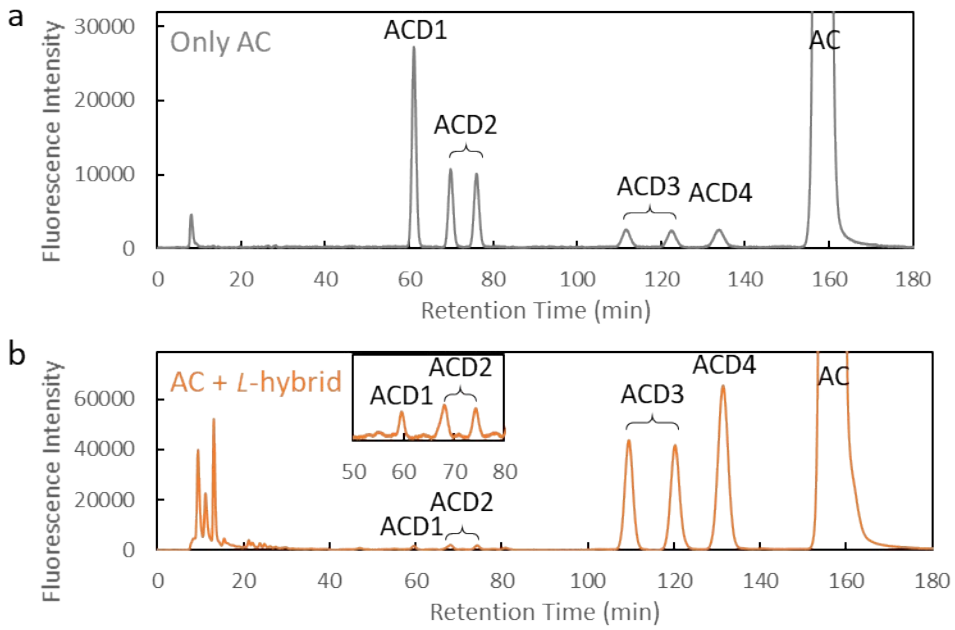

Fig. S1 The HPLC chromatogram of the products from (a) [4+4] cyclodimerisation of AC in buffer pH 7 and (b) supramolecular regioselective [4+4] cyclodimerisation of AC with L-hybrid nanoribbons.

Spectroscopic Data

Time-Dependent Circular Dichroism Spectroscopy

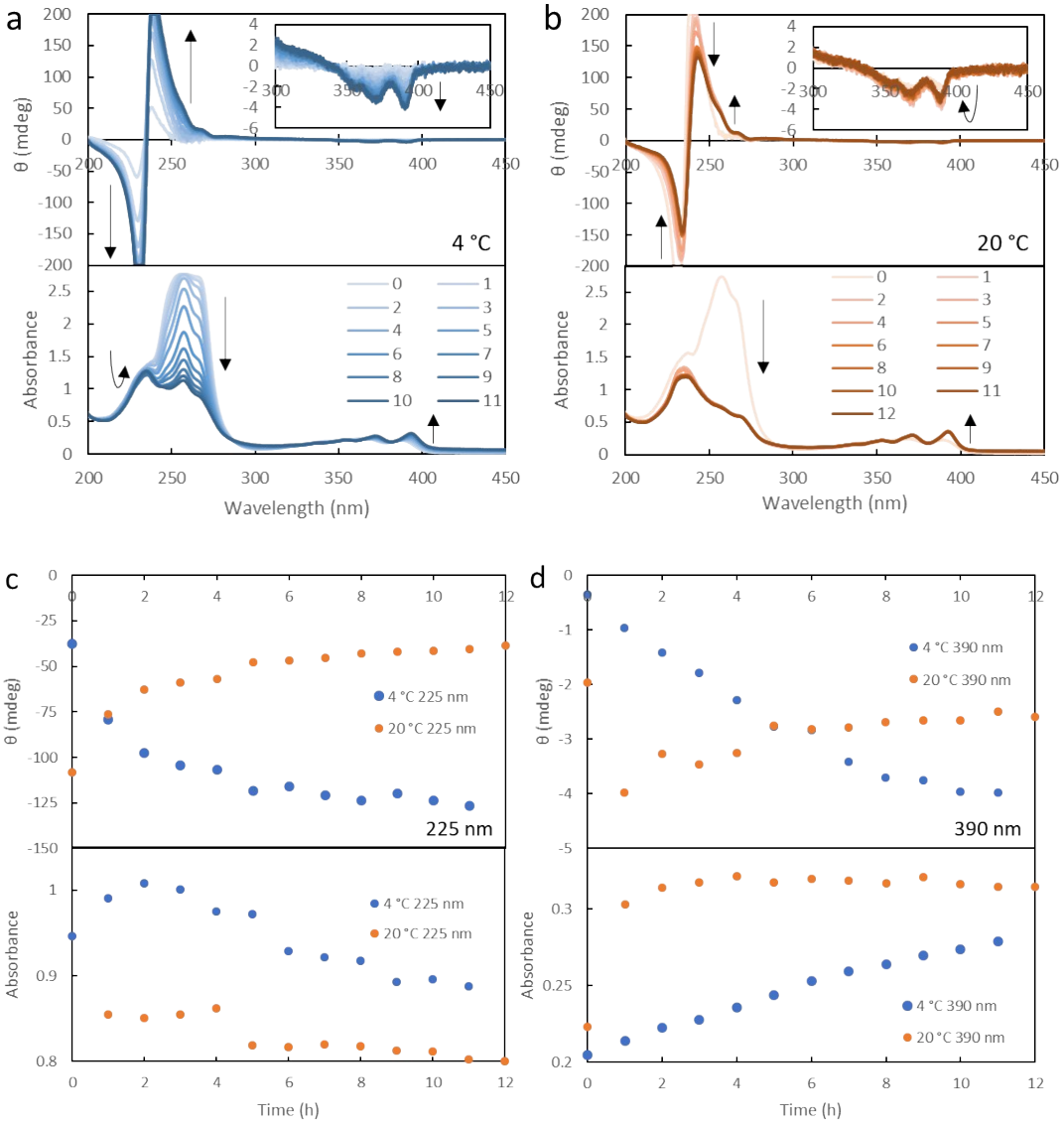

Fig. S2 The time-dependent CD and UV-Vis spectra of a mixture of AC (50 µM) and L-hybrid nanoribbons (50 µM) at (a) 4 °C and (b) 20 °C, and the plots of CD intensity and absorbance at (c) 225 nm and (d) 390 nm, measured at 4 °C (blue) and 20 °C (orange).

The progress of exchange of the tartrate in nanoribbon with AC was monitored by time-dependent UV-Vis and CD spectra to find the optimum time for the maximum and stable CD intensity, which is necessary for ensuring the reproducibility and consistency in all the experiments. The measurements were conducted using the time-dependent measurement program of the CD spectrometer. The parameters were the same as the other CD measurements, excepting the use of a single scan instead of the quadruple scans in the standard measurements. The AC and hybrid nanoribbons

(in the ice bath for 4 °C and at room temperature for 20 °C) were mixed in the quartz cell and immediately placed in the CD spectrometer. The holder was preset at 4 or 20 °C. The solution was stirred constantly throughout the measurement (Fig. S2). The absorption peak at 387 nm of AC was significantly red-shifted to 394 nm, indicating J-aggregation of AC inside the hybrid nanoribbons (Fig. S2 a).

Circular Dichroism Titration Between AC and Hybrid Nanoribbons

A stock solution of AC was prepared by dissolving AC in 1 mM NaOH solution (5 mL) and then filtered through 0.2 µm membrane filter; the final concentration was determined from the absorbance of AC. The **16-2-16** tartrate was mixed with a given quantity of the stock solution of AC on a roller mixer. The exchange of tartrate in hybrid nanoribbons with AC was monitored by UV-Vis and CD spectroscopies (Fig. S3).

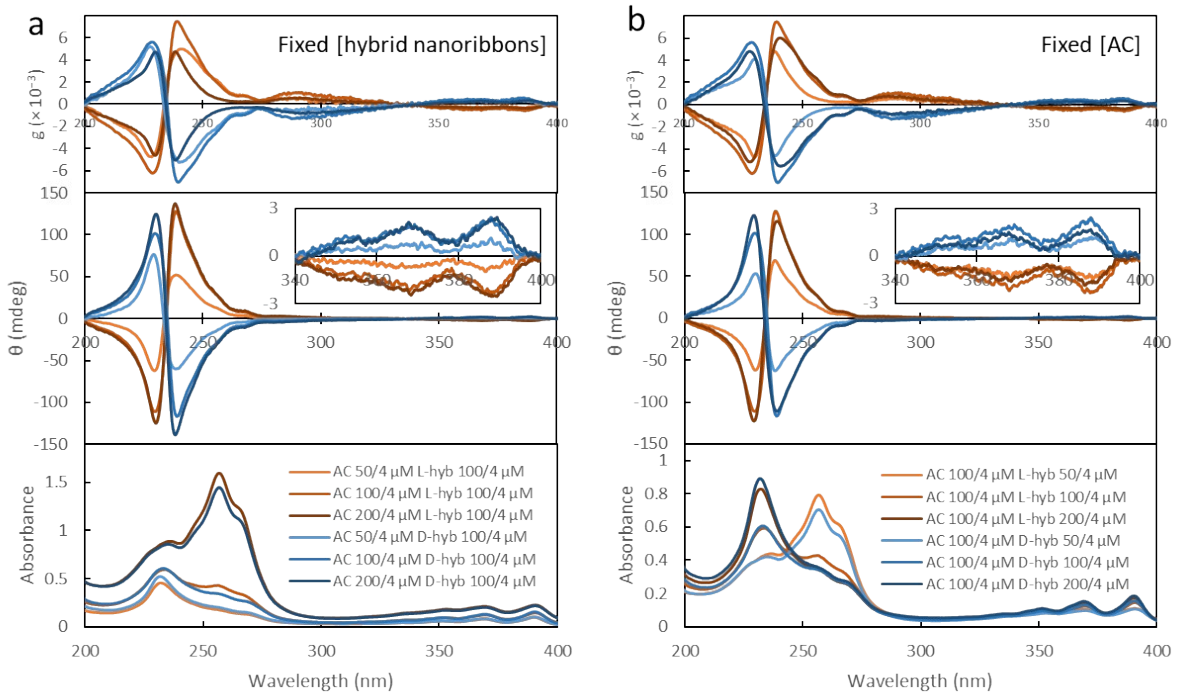

Fig. S3 The CD and absorption spectra of AC-exchanged L-hybrid ribbons in different ratios, and the g-factors calculated from them. (a) The AC (50, 100 and 200 µM) was varied with fixed L-hybrid ribbons (100 µM), and (b) vice versa. All suspensions were incubated at 4 °C for 16 h on roller mixer, and they were diluted to ¼ of the original concentration before the measurement.

Negligible Induced Linear Dichroism of AC in Hybrid Nanoribbons

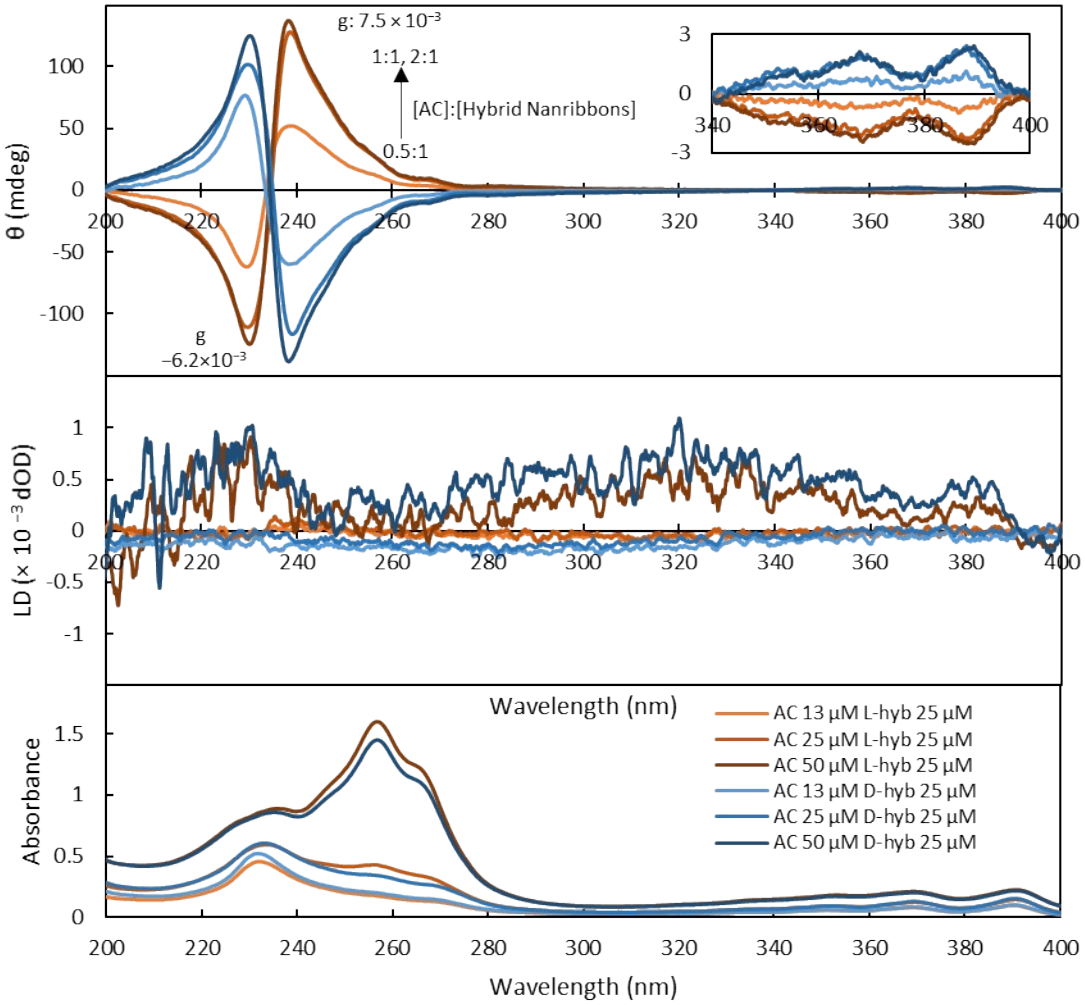

Fig. S4 The CD, LD and absorption spectra of AC (50, 100 and 200 μM) in L-hybrid ribbons (100 μM). All suspensions were incubated at 4 °C for 16 h on roller mixer, and they were diluted to ¼ of the original concentration before measurement.

It is known that linear dichroism (LD) is a common component originating from asymmetric alignment or asymmetric diffusions of macroscopic system in solutions. In our system, the ellipticity from LD phenomena in every CD measurement was checked experimentally. The solution is stirred during measurement, and LD spectra were measured, following by CD spectra. Fig. S4 is one example of LD spectra with CD spectra. All the LD spectra reach to the conclusion that LD contribution is negligible in our measurement.

Fluorescence Spectroscopy of AC and Hybrid Nanoribbons

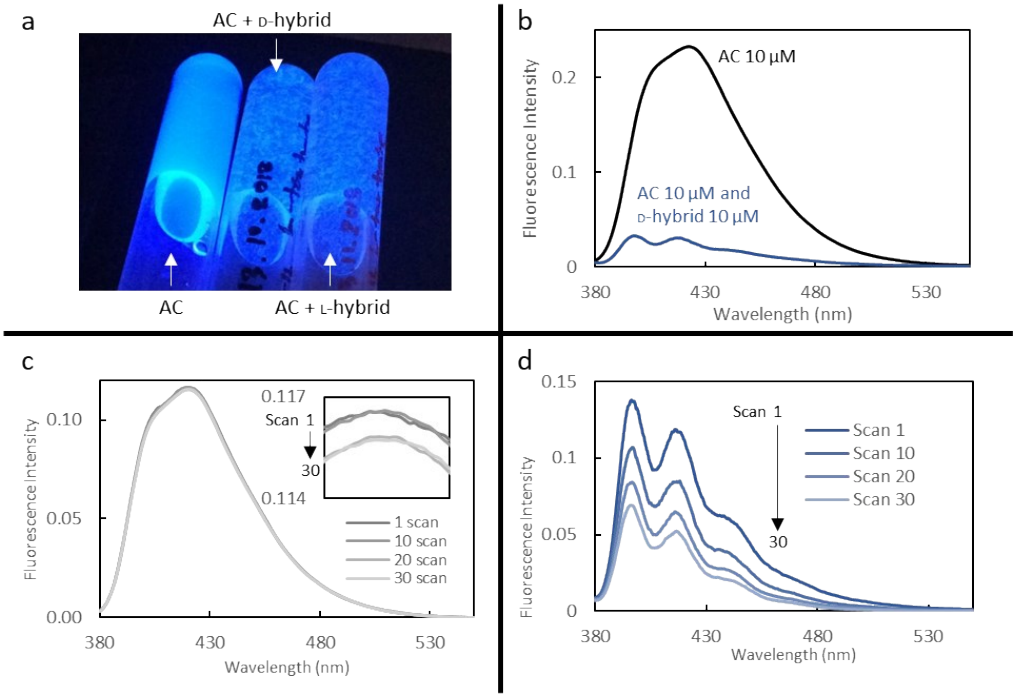

Fig. S5 The fluorescence emission spectra of (a) AC (100 mM) with and without hybrid nanoribbons (100 mM) observed under a 352 nm UV lamp, (b) AC (10 mM) with and without D -hybrid nanoribbons (10 mM) (JASCO CPL-300, ex 350 nm, ex and em bandwidth 10 nm, detector HT 800 V, scan speed 100 nm/s), (c) AC (10 mM) after multiple scans (the same parameter as (b), except for the detector HT 700 V), (d) AC (10 mM) with D-hybrid nanoribbons (10 mM) after multiple scans (the same parameters as (b), except for the detector HT 850 V).

Infrared and Vibration Circular Dichroism Spectroscopy

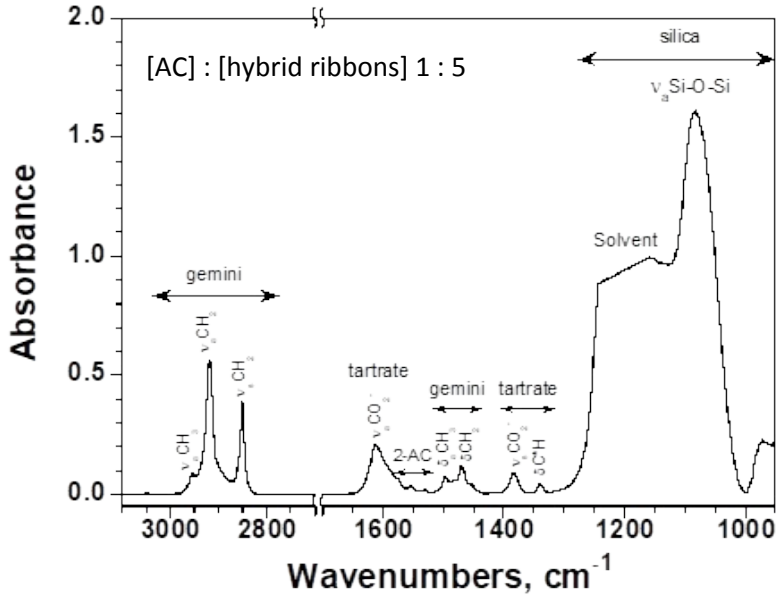

Fig. S6 The IR spectrum of hybrid nanoribbons of AC-exchanged **16-2-16** L-tartrate (1 : 5) in D_2O solution.

The IR spectrum of hybrid nanoribbons of AC-exchanged **16-2-16** L-tartrate (1 : 5) in D_2O is shown as a typical example (Fig. S6) in the 3100-950 cm^{-1} spectral range. This IR spectrum exhibits bands related to the different constituents of the hybrid nanoribbons, i.e. **16-2-16**, L-tartrate, AC and silica. The **16-2-16** is characterised by the antisymmetric (ν_aCH_2) and symmetric (ν_sCH_2) stretching modes of the methylene groups at 2919 and 2850 cm^{-1}, respectively, by the antisymmetric (ν_aCH_3) stretching modes of the methyl groups at 2955 cm^{-1}, and by the bending modes of methyl (δ_aCH_3, $\delta_{s'}CH_3$ and δ_sCH_3) and methylene (δCH_2) groups in the 1510-1420 cm^{-1} region.[3] The frequencies obtained for the ν_aCH_2 (ca 2919 cm^{-1}) and ν_sCH_2 (ca 2850 cm^{-1}) modes along with the δCH_2 mode which shows a splitting (ca 1470 and 1466 cm^{-1}) indicate that the alkyl chains are well organised in an orthogonal packing with mainly an all *trans* conformation. The L-tartrate is characterised by the antisymmetric ($\nu_aCO_2^-$) and symmetric ($\nu_sCO_2^-$) stretching modes of the carboxylate groups at 1611 and 1384 cm^{-1}, respectively, and by the bending mode of the C*H group at 1340 cm^{-1}.[3] The AC is characterised by several bands in the 1650-1510 cm^{-1} spectral range, related to carboxylate (1584 and 1414 cm^{-1}) and νC=C stretching modes of anthracene (1627, 1572, 1552 and 1530 cm^{-1}).[4,5] Finally, the silica is characterised by the strong band at 1082 cm^{-1}, associated with the transverse optic (TO) mode of the asymmetric (ν_aSi-O-Si) stretching vibration of Si-O-Si groups.[6] The band at 970 cm^{-1} can be assigned to the Si-OH stretching vibration of free silanol groups.

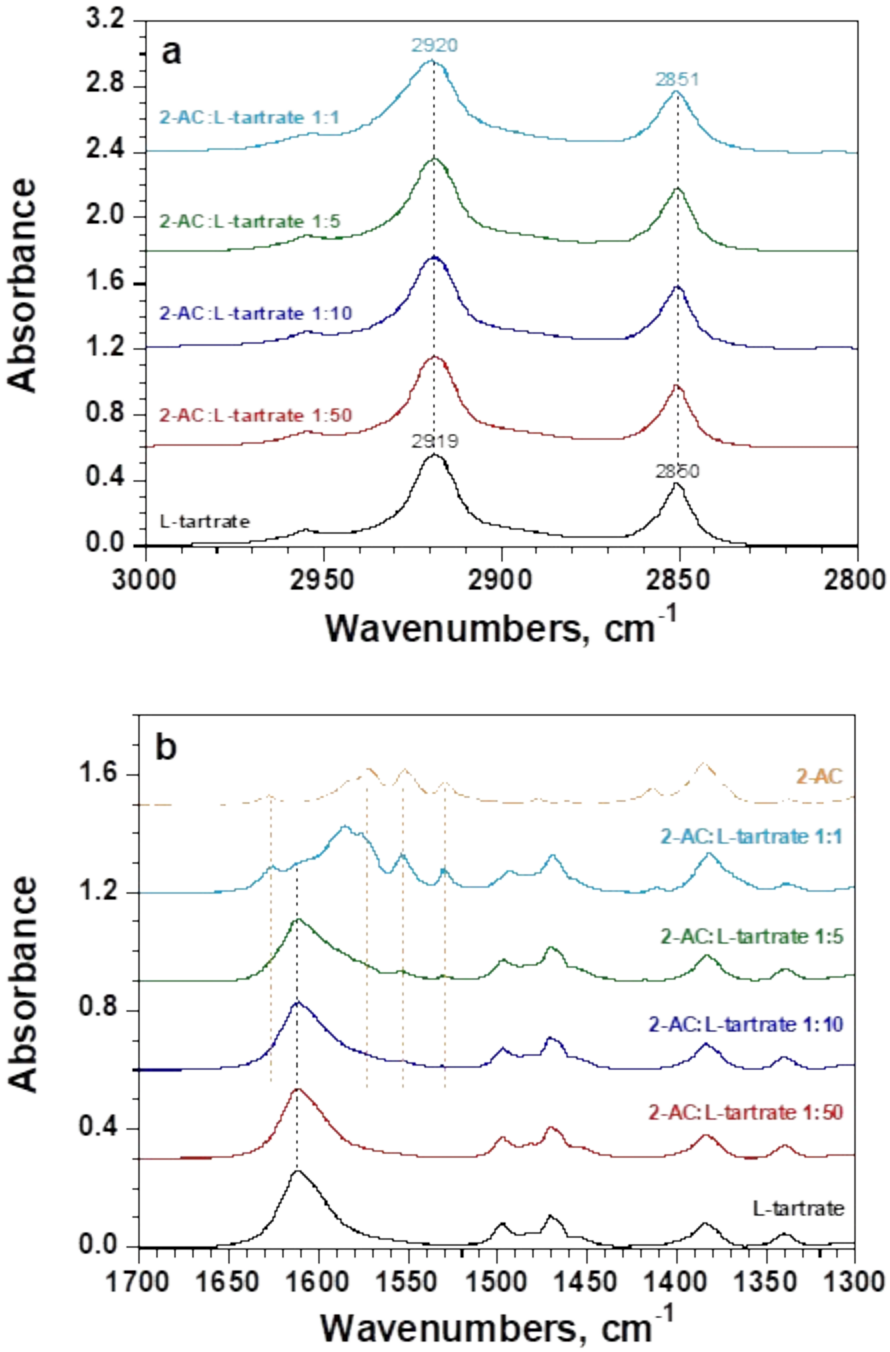

Fig. S7 The IR spectra of of AC-exchanged L-hybrid nanoribbons in different proportions ([AC] : [hybrid nanoribbons] = 1 : 1, 1 : 5, 1 : 10 and 1 : 50) in D_2O solution as well as the IR spectra of L-hybrid nanoribbons and sodium salt of AC in (a) the 3000-2800 cm^{-1} and (b) 1700-1300 cm^{-1} spectral ranges.

The IR spectra of hybrid nanoribbons of AC-exchanged 16-2-16 L-tartrate in different proportions ([AC] : [hybrid] = 1 : 1, 1 : 5, 1 : 10 and 1 : 50) in D_2O solution as well as the IR spectra of L-hybrid nanoribbons and of sodium salt of AC are presented in Fig. S7a and b in the 3000-2800 cm^{-1} and 1700-1300 cm^{-1} spectral ranges, respectively. Fig. S7 show that the organisation of the alkyl chains of **16-2-16**, in an orthogonal packing with mainly an all *trans* conformation, is not modified by the exchange of tartrate

with AC. Indeed, any modification of the frequencies for the ν_aCH_2 (*ca.* 2919 cm^{-1}) and ν_sCH_2 (*ca.* 2850 cm^{-1}) modes is observed when the proportion of AC increases and the splitting of the δCH_2 mode is always present at 1470 and 1466 cm^{-1}. Only a very low broadening of the ν_aCH_2 and ν_sCH_2 bands associated with a shift by one wavenumber at higher frequencies are observed for the [AC] : [tartrate] = 1 : 1 sample.

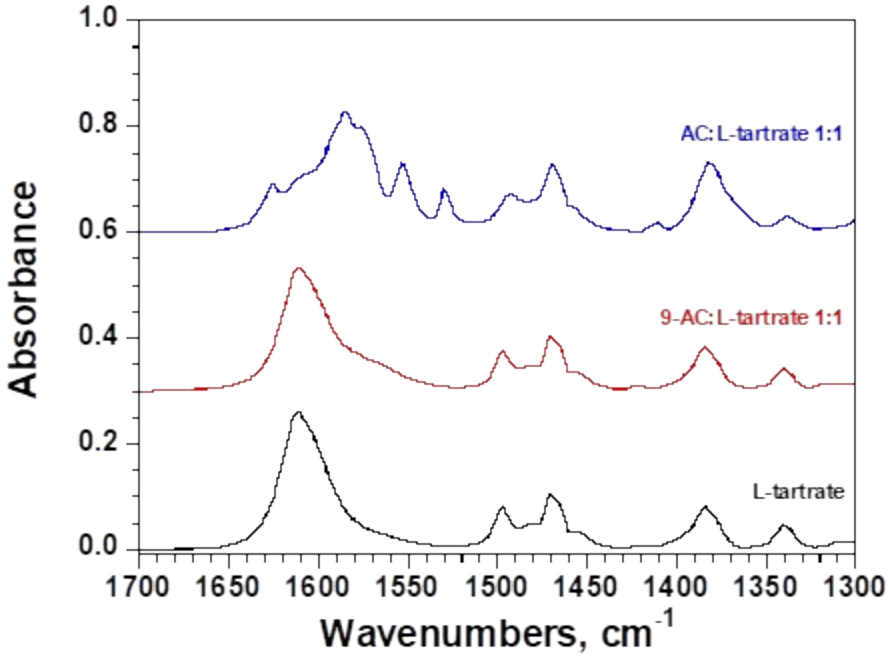

Fig. S8 The IR spectra of L-hybrid nanoribbons (black), 9-AC-exchanged **16-2-16** L-tartrate (1 : 1) (red) and AC-exchanged **16-2-16** L-tartrate (1 : 1) (blue) in D_2O in the 1700-1300 cm^{-1} spectral range.

The comparison between the exchangeability of AC and 9-anthracenecarboxylate (9-AC) was studied. The IR spectra (Fig. S8) of L-hybrid nanoribbons (black), 9-AC-exchanged **16-2-16** L-tartrate (1 : 1) (red) AC-exchanged **16-2-16** L-tartrate (1 : 1) (blue) in D_2O in the 1700-1300 cm^{-1} spectral range were recorded. The black and red spectra are very similar, revealing that the exchange of tartrate with 9-AC did not occur (or occurred in relatively much low efficiency). The carboxylate group must be at one end of the anthracene to promote the efficient exchange with tartrate.

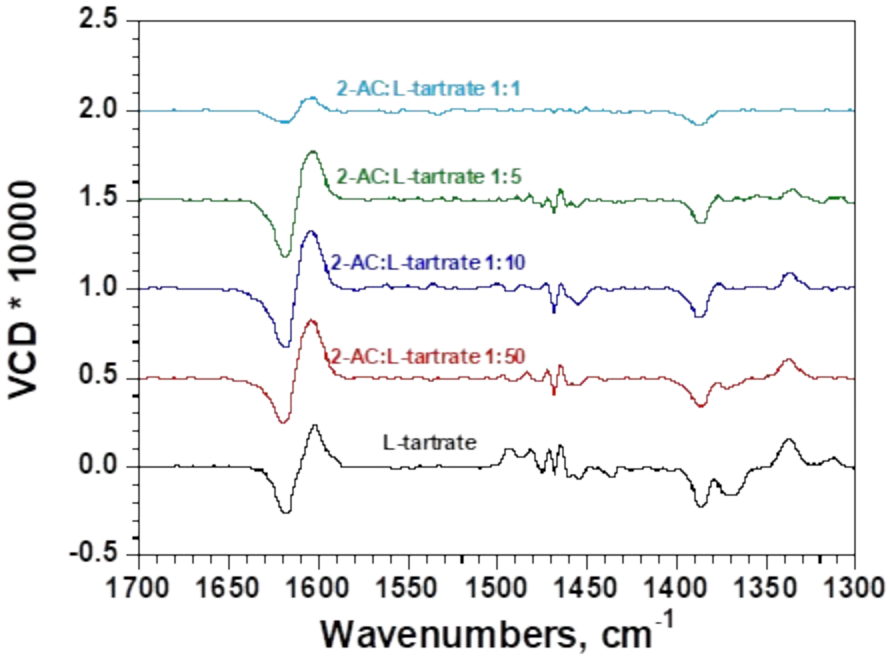

Fig. S9 The VCD spectra of hybrid nanoribbons of AC-exchanged **16-2-16** L-tartrate in different proportions ([AC] : [hybrid nanoribbons] = 1 : 1, 1 : 5, 1 : 10 and 1 : 50) in D_2O as well as the VCD spectra of L-hybrid nanoribbons in the 1700-1300 cm^{-1} spectral range.

The VCD spectra of hybrid nanoribbons of AC-exchanged **16-2-16** L-tartrate in different proportions ([AC] : [hybrid nanoribbons] = 1 : 1, 1 : 5, 1 : 10 and 1 : 50) in D_2O as well as the VCD spectra of L-hybrid nanoribbons are presented in Fig. S9 in the 1700-1300 cm^{-1} spectral range. The VCD spectrum of organic **16-2-16** L-tartrate has already been reported.[3] This spectrum exhibits a bisignate band for the $\nu_a CO_2^-$ mode (positive couplet for **16-2-16** L-tartrate) and a negative band for the $\nu_s CO_2^-$ mode. The VCD spectrum reveals also the chiral induction from tartrate to non-chiral gemini surfactant. Indeed, a (+, −, +) pattern is observed for the two split components of the bending (δCH_2) mode of methylene groups located at 1470 and 1466 cm^{-1}. The VCD spectrum of L-hybrid nanoribbons is similar to the one of **16-2-16** L-tartrate the 1700-1300 cm^{-1} spectral range. Moreover, this spectrum is slightly modified by the exchange of L-tartrate with AC, except of the 1 : 1 composition. Indeed, a marked diminution of the VCD intensities is observed for this composition, revealing certainly a modification in the chiral structure of the supramolecular assemblies. In contrast, the AC at certain lower ratios enlarged the VCD intensities of tartrate, which might indicate more rigid chiral assemblies.

Circular Dichroism and UV-Vis Spectra After Photoirradiation

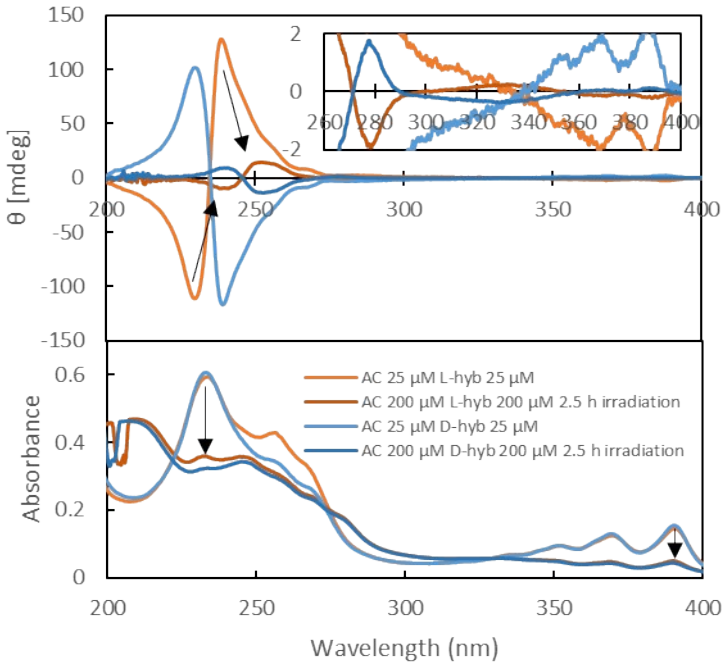

Fig. S10 The CD and absorption spectra of AC-exchanged hybrid nanoribbons before and after irradiation. Note that the spectra before the irradiation was from 25 µM, while the spectra after the irradiation was 200 µM

After the irradiation, the intensity of absorption spectra decreased significantly, especially at 350 - 400 nm, indicating the diminishing of AC. The shape of the spectrum also changed. The CD intensity immensely decreased throughout the spectrum. The shape of the CD also changed. (Fig. S10)

Approximation of AC Photocyclodimerisation Rates

Due to its bimolecular nature, the photocyclodimerisation of AC should follow the second-order kinetics:

$$\text{AC*} + \text{AC} \rightarrow \textbf{ACD}$$

where AC* denotes electronically excited AC molecule, and **ACD** denotes the isomeric AC dimers. Assuming reaction rate (*r*) and rate constant (*k*) are the same for all **ACD**s, the reaction rate can be expressed by

$$r = k[AC^*][AC] = \frac{d[ACD]}{dt} \tag{1}$$

where *t* denotes time. The formation of **ACD** is equal to the consumption of AC or AC*.

$$[ACD] = [AC^*]_0 - [AC^*] = [AC]_0 - [AC]$$

Hence, $$[AC^*] = [AC^*]_0 - [ACD] \text{ and } [AC] = [AC]_0 - [ACD] \tag{2}$$

By substituting equation (2) to equation (1) and solving the differential equation, the following equation is derived.

$$\ln\left(\frac{[AC]}{[AC^*]} \cdot \frac{[AC^*]_0}{[AC]_0}\right) = \left([AC]_0 - [AC^*]_0\right)kt \tag{3}$$

Under the conventional photoirradiation conditions with a noncoherent light source, the [AC*] in the solution is approximated to be much lower than [AC], so the following assumption can be deduced.

$$[AC^*] << [AC]$$

Therefore,

$$[AC] \approx [AC]_0$$

The equation (3) can be approximated as:

$$\ln\left(\frac{[AC^*]_0}{[AC^*]}\right) = [AC]_0 kt$$

$$\ln[AC^*]_0 - ln[AC^*] = [AC]_0 kt$$

$$\ln[AC^*] = -[AC]_0 kt + ln[AC^*]_0 \tag{4}$$

This variation is called pseudo-first-order reaction, a useful approximation for the second-order reaction when one of the reactants has much higher concentration than the other. Because the concentration of AC is low (10^{-5} M) and the fluorescence quantum yield is lowered by the reaction, the fluorescence emission intensity (I_{FL}) is approximately a direct variation of [AC*].

$$a \cdot I_{FL} = [AC^*]$$

When a is a constant, the equation (4) can be rewritten as:

$$\ln I_{FL} = -[AC]_0 kt + ln\frac{[AC^*]_0}{a} = -[AC]_0 kt + b \quad (5)$$

when b is a constant. As a result, by plotting ln I_{FL} versus time, k can be calculated from −slope/$[AC]_0$.

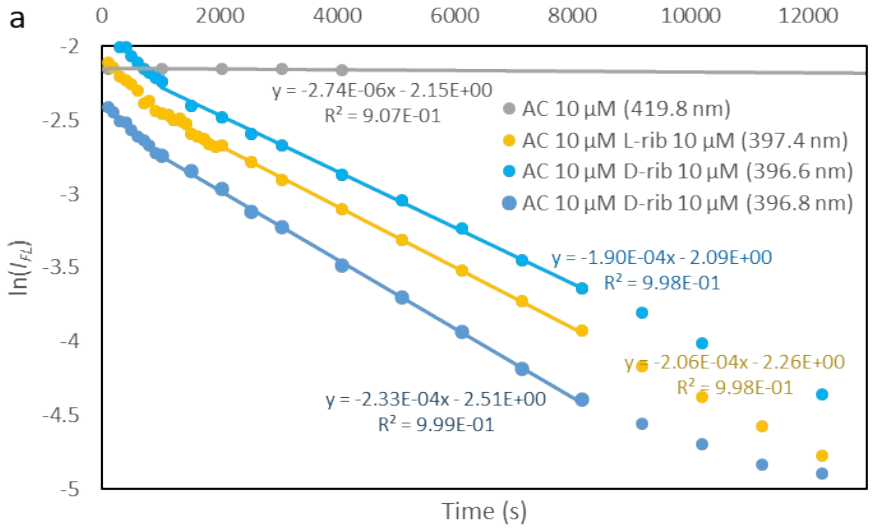

Fig. S11 The graph of ln(I_{FL}) versus time of AC (10 µM) alone (grey) and with L- and D-hybrid nanoribbons (10 µM) (yellow and blue, respectively). The ln(I_{FL}) was calculated using the maximum I_{FL} of each sample.

The plot of natural logarithm of fluorescence emission intensity at 397 nm versus time (Fig. S11) shows almost linear relationship over 2 h. Although the data taken from CPL is intensity versus scanning round, the time of each scan (102 s) was calculated from the known scanning speed (100 nm/min) and scanning range (380 - 550 nm). For the AC solution, the linear progression functions were fitted to 1st, 10th, 20th, 30th and 40th scan. The linear regression function is fitted with the R^2 of 0.91 because the change is too minimal, so that the detection error affects the calculation. The k was 2.74 × 10^{-1} $M^{-1}s^{-1}$.

For the AC-exchanged hybrid nanoribbons, the data from 1000 to 9000 s range, which is the closest range to linear, was used to calculate k. The linear regression functions were fitted with the minimum R^2 of 0.98. The average of k was 2.10 (± 0.22) × 10^{1} $M^{-1}s^{-1}$, 2 order of magnitude higher than of free AC in solution, indicating a significant acceleration.

Different Exchange of AC and Halide to Tartrate in Hybrid Nanoribbons

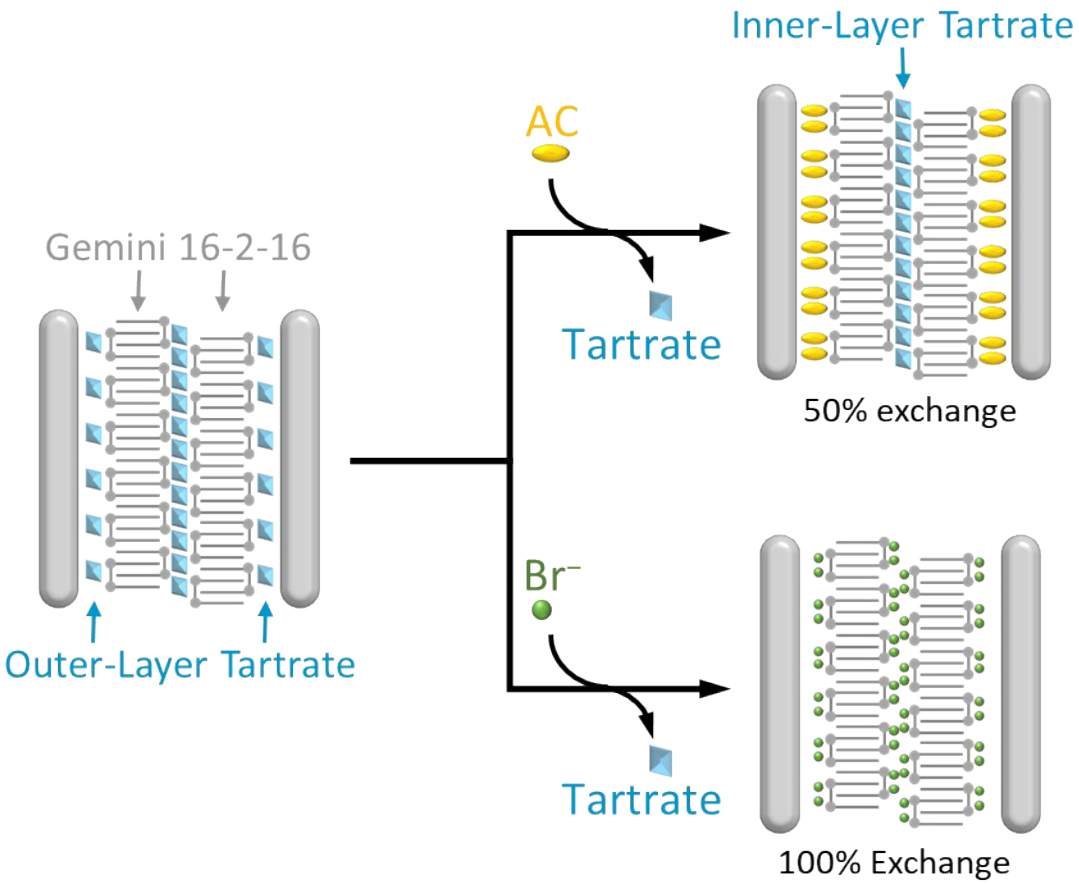

Fig. S12 The difference between the exchange of tartrate to AC and bromide (halide).

The previous work has reported that tartrate can be totally exchanged with halide anions (Cl^- or Br^-) with minimal perturbation of gemini crystalline structure, evidently from VCD spectra.[7,8] However, AC shows maximum CD at 1 to 1 ratio, meaning only half of tartrate can be easily exchanged by AC.

References

1 T. Buffeteau, F. Lagugné-Labarthet and C. Sourisseau, *Appl. Spectrosc.*, 2005, **59**, 732–745.

2 L. A. Nafie and D. W. Vidrine, in *Fourier Transform Infrared Spectroscopy*, eds. J. . Ferraro and L. J. Basile, Academic Press, New York, 1982, pp. 83–123.

3 A. Brizard, D. Berthier, C. Aimé, T. Buffeteau, D. Cavagnat, L. Ducasse, I. Huc and R. Oda, *Chirality*, 2009, **21**, E153–E162.

4 J. G. Radziszewski and J. Michl, *J. Chem. Phys.*, 1985, **82**, 3527–3533.

5 F. Cataldo, D. A. García-Hernández and A. Manchado, *Fullerenes Nanotub. Carbon Nanostructures*, 2014, **22**, 565–574.

6 Y. Okazaki, T. Buffeteau, E. Siurdyban, D. Talaga, N. Ryu, R. Yagi, E. Pouget, M. Takafuji, H. Ihara and R. Oda, *Nano Lett.*, 2016, **16**, 6411–6415.

7 N. Ryu, Y. Okazaki, E. Pouget, M. Takafuji, S. Nagaoka, H. Ihara and R. Oda, *Chem. Commun.*, 2017, **53**, 8870–8873.

8 Y. Okazaki, N. Ryu, T. Buffeteau, S. Pathan, S. Nagaoka, E. Pouget, S. Nlate, H. Ihara and R. Oda, *Chem. Commun.*, 2018, **54**, 10244–10247.